

CHAPTER 2

IONOSPHERIC PROPAGATION

2.1 INTRODUCTION

Long-distance transmission in the HF band depends entirely upon refraction of radio waves by the ionosphere, a region in the upper atmosphere where free electrons are produced by the ionizing effect of ultraviolet light and soft x-rays from the sun. Under favorable conditions, a radio wave reaching the ionosphere will be bent earthward and may return to earth at a great distance from the transmitter.

Radio waves that follow such a path through the ionosphere and back to earth are known as sky waves and are often spoken of as being reflected by the ionosphere. Although this concept of the mechanics of sky-wave propagation is practical in terms of the end result, the dominant physical phenomenon is refraction, not reflection. The electron density varies gradually, rather than abruptly, with height, and this causes radio waves to follow curved paths through the ionosphere instead of being reflected in a manner analogous to reflection of light from a mirror.

Since many of the complexities of ionospheric propagation have no practical role in long term circuit planning, a comprehensive treatment of the subject is not attempted here. Rather, this discussion is intended as background or refresher material to foster understanding of the prediction procedures described later in this chapter. Reference 2 is an excellent text for those who wish to pursue the subject in greater depth.

2.2 STRUCTURE OF THE IONOSPHERE

Ionization density in the ionosphere tends to peak at various heights above the earth as a result of differences in the physical properties of the atmosphere at different heights. The levels at which the electron density reaches a maximum are termed layers and these are identified as the D, E, F1 and F2 layers in order of increasing height and ionization density. The relative distribution of these layers above the earth is shown in figure 2-1. The number of layers, their heights, and their ionization (electron) density vary both geographically and with time.

2.2.1 D Layer

The D layer lies between heights of about 30 and 55 miles above the earth, and absorption in this layer is the principal cause of the daytime attenuation of high-frequency sky waves. The D layer exists only in the daylight hours and its ionization density correlates with the elevation angle of the sun. Compared to the other layers at higher altitudes the electron density is relatively low, but the free electrons are excited by the presence of an electromagnetic wave, and pronounced energy losses occur because of collisions between the electrons and the molecules of the atmosphere. The refractive index is so near unity that little or no bending of radio waves takes place.

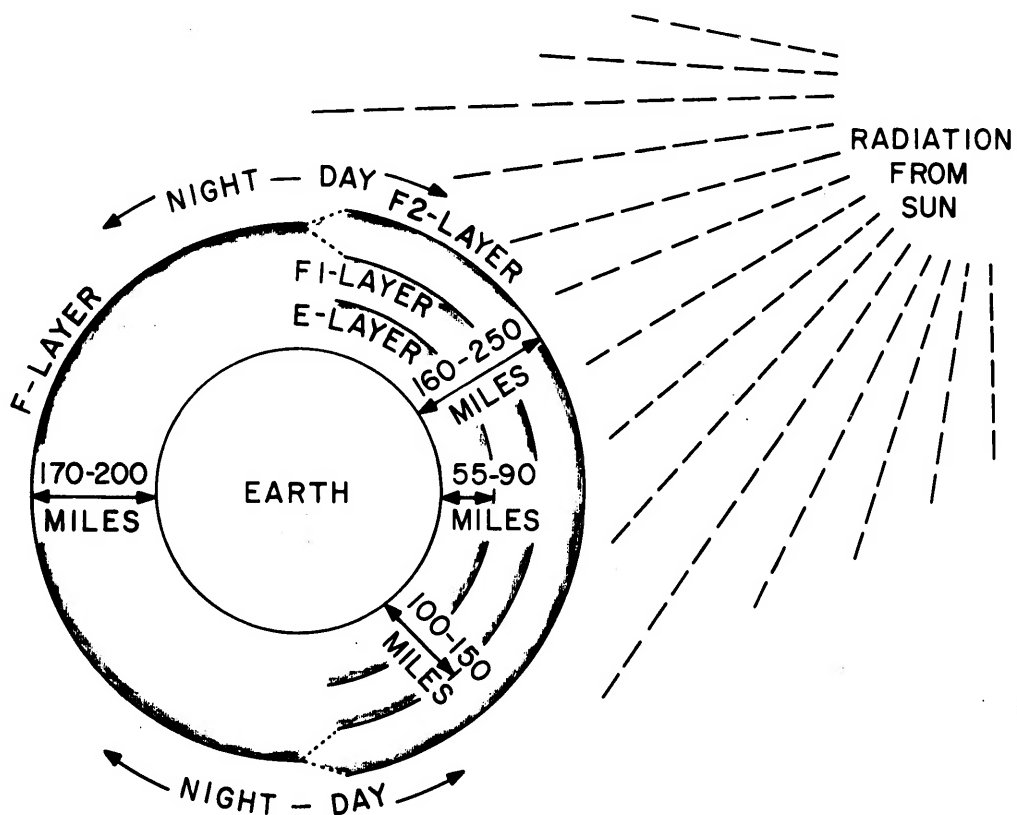


Figure 2-1. Distribution of Layers in the Ionosphere

2.2.2 E Layer

The E layer, the second layer in order of height, exists between 55 and 90 miles above the earth's surface with maximum density relatively constant at about 70 miles. This layer is sometimes called the Kennelly-Heaviside region, after the names of the men who first proposed its existence. The variations of this layer are regular and quite predictable. The intensity of ionization follows the sun's altitude closely, reaching a maximum about noon, and fading to such a weak level during the night as to be practically useless as an aid to HF radio communication. The density of electrons in the E layer is usually great enough to refract to earth radio waves at frequencies as high as 20 MHz. The height of this layer and its refractive properties make it important for HF daytime propagation at distances less than approximately 1200 miles. Longer distance transmission via the E layer is usually impractical because of the low layer height and correspondingly low vertical angle of departure of the transmitted wave. With this geometry, multiple reflections between the E layer and the earth's surface

are required for long distance transmission, and a wave following such a path suffers pronounced absorption during its travel through both the D and E layers.

2.2.3 F Region

For HF radio communications, the F region is the most important part of the ionosphere. Long-term studies of the structure of the F region by remote probing techniques show conclusively the existence of two distinct layers, called the F1 and F2 layers. These two merge at night into a single F layer at a height of 170 to 200 miles. During the day the F1 layer has a lower limit of approximately 100 miles, while the F2 layer has a lower limit of about 160 to 250 miles depending upon the season of the year and the time of the day.

a. F1 Layer. The F1 layer has not been as well defined as the F2 layer in terms of its predictable characteristics. This layer occasionally is the refracting region for HF transmission, but usually oblique-incidence waves that penetrate the E layer also penetrate the F1 layer and are bent earthward by the F2 layer. The principal effect of the F1 layer is to introduce additional absorption of such waves.

b. F2 Layer. The F2 layer is by far the most important layer for HF radio communications, and, unfortunately, it is also the most variable. It is the most highly ionized of all the layers and its height and ionization density vary diurnally, seasonally and over the 11-year sunspot cycle. The degree of ionization does not follow the altitude of the sun in any simple fashion but it generally peaks in the afternoon and decreases gradually throughout the night. The absence of the F1 layer at night, and reduction in absorption in the E layer, cause nighttime signal intensities (and noise) to be generally higher than they are during daylight hours.

2.3 SKY-WAVE PROPAGATION

2.3.1 Refraction of Radio Waves

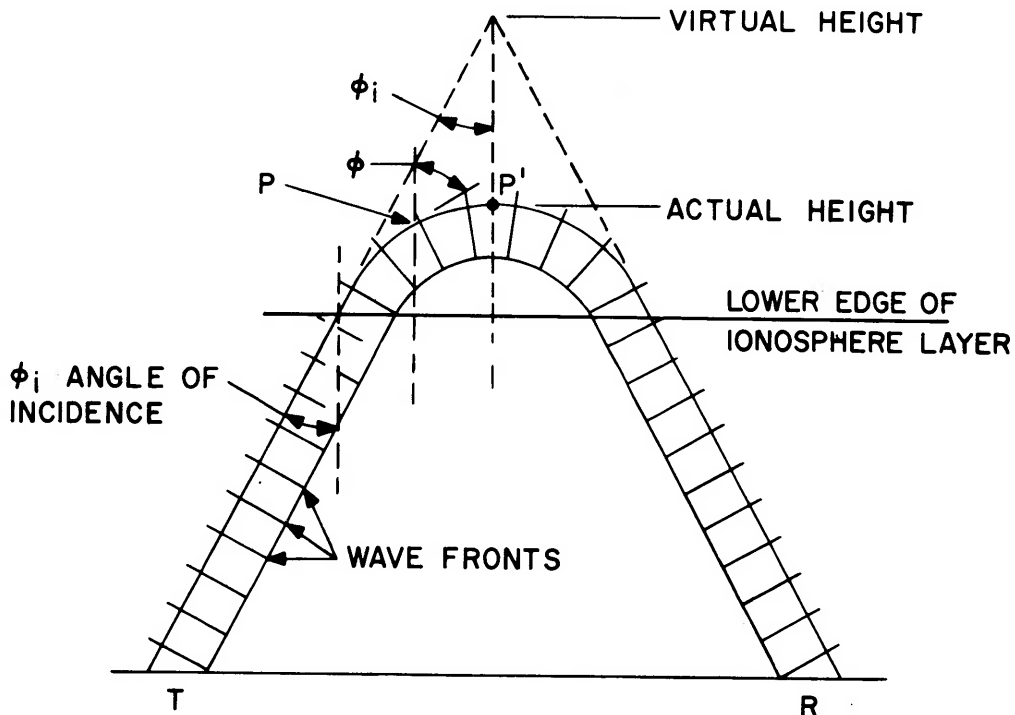
A radio wave traveling through the ionosphere obeys ordinary optical laws and, consequently, follows a curved path. Free electrons in the ionosphere reduce the refractive index below that of the atmosphere so that the path of a radio wave bends away from regions of high electron density toward regions of lower electron density. The refractive index is related to electron density by the following expression:

$$n = \sqrt{1 - \frac{81N}{f^2}} \quad (2-1)$$

where n = refractive index
 N = number of electrons per cc
 f = frequency, kHz

It is apparent from equation (2-1) that the refractive index is not a constant, but rather a variable depending upon the frequency of the wave and the change of electron density through the ionosphere. Since, for a given ionospheric layer, the electron density increases with height to a maximum and then decreases, the refractive index decreases with height to a minimum and then increases. Consequently, since the phase velocity of a radio wave is inversely proportional to the refractive index, the part of the wavefront

at a height of low refractive index travels faster than the portion of the wavefront at a height of higher refractive index. This causes the wave path to bend as shown in figure 2-2.



LEGEND:

ϕ = ANGLE OF REFRACTION AT ANY POINT P

ϕ_i = ANGLE OF INCIDENCE AT THE LOWER
EDGE OF THE IONOSPHERE

P' = TOP OF THE PATH WHERE $O = 90^\circ$

Figure 2-2. Refraction of a Radio Wave

This bending of a radio-wave path caused by the ionosphere depends also upon the angle of incidence according to Snell's law,

$$n \sin \phi = \sin \phi_i \quad (2-2)$$

where n = refractive index of any point P (figure 2-2)

ϕ = angle of refraction of any point P

ϕ_i = angle of incidence at the lower edge of the ionosphere

Equations (2-1) and (2-2) indicate that the path of a wave through the ionosphere is determined by the frequency of the incident wave, its angle of incidence and the refractive index.

For a given frequency, the smaller the angle of incidence (the more nearly vertical the wave) the lower the refractive index (the higher the electron density) required to return the wave to earth. For a given angle of incidence, the higher the frequency, the deeper will be the penetration of the wave into the ionosphere. That is, the higher the frequency, the greater the electron density required to refract the wave earthward.

At the top of the path, point P' in figure 2-2, where $\theta = 90^\circ$, equation 2-2 becomes

$$n = \sin\theta_i \quad (2-3)$$

The relationship of equation (203) must be satisfied if a wave reaching the ionosphere is to be returned to earth. If the refractive index is too great to satisfy this relationship for the frequency and angle of incidence involved, the wave path will not be curved sufficiently to return to earth.

2.3.2 Critical Frequency, MUF, FOT

Depending on the electron density at each layer, there is a highest frequency, termed the critical frequency, at which the layer returns a vertically incident wave. At vertical incidence, $\theta_i = 0$ in equation 2-3, and, therefore, for a vertically incident wave to be returned to earth, the electron density at some point in a layer must be sufficient to reduce the refractive index to zero. The critical frequency for a layer is the frequency for which this point of zero refractive index is reached at the height of the maximum electron density of the layer. If the maximum electron density is too low for a given frequency, the radio wave will pass on through the layer.

Waves of critical and lower frequencies will be reflected from the layer regardless of the angle of incidence. Waves of a frequency higher than the critical frequency will be reflected at oblique incidence only if the angle of incidence is large enough to satisfy equation (2-3) at the frequency involved. The highest frequency that can be propagated in this way over a given path between specified terminals is called the maximum usable frequency (MUF).

The MUF will vary as ionospheric conditions over the path change. In particular, the highly variable characteristics of the F2 layer cause the F2-layer MUF to vary appreciably from the values given by propagation prediction services. Predictions of MUF are made for the monthly median value, the value equaled or exceeded 50 percent of the days during the month at a specified time of day. Consequently, the MUF is not a practical operating frequency for propagation via the F2 layer. A lower frequency, 0.85 times the MUF, is taken as a practical value that will be equaled or exceeded 90 percent of the days during the month. This frequency has been called the optimum working frequency or optimum traffic frequency and is abbreviated FOT. (The international abbreviation, FOT, is formed from the initial letters of the French words for optimum working frequency, "Frequence Optimum de Travail.") This 85 percent limit provides some margin for ionospheric irregularities as well as for day-to-day deviations from the monthly median MUF.

The day-to-day variations of the E-layer MUF and the F1-layer MUF can be considered negligible for operational use. Because of the stability of the E and F1 layers, no adjustment is made such as that above and the monthly median MUF is used as the FOT for these layers.

2.3.3 Ray Paths and Skip Distance

Figure 2-3 illustrates the effect of the ionosphere on the path of a radio wave of a given frequency as the angle of incidence is varied. When the angle of incidence is relatively large (ray 1), the propagation path is long and the wave is returned to earth after only

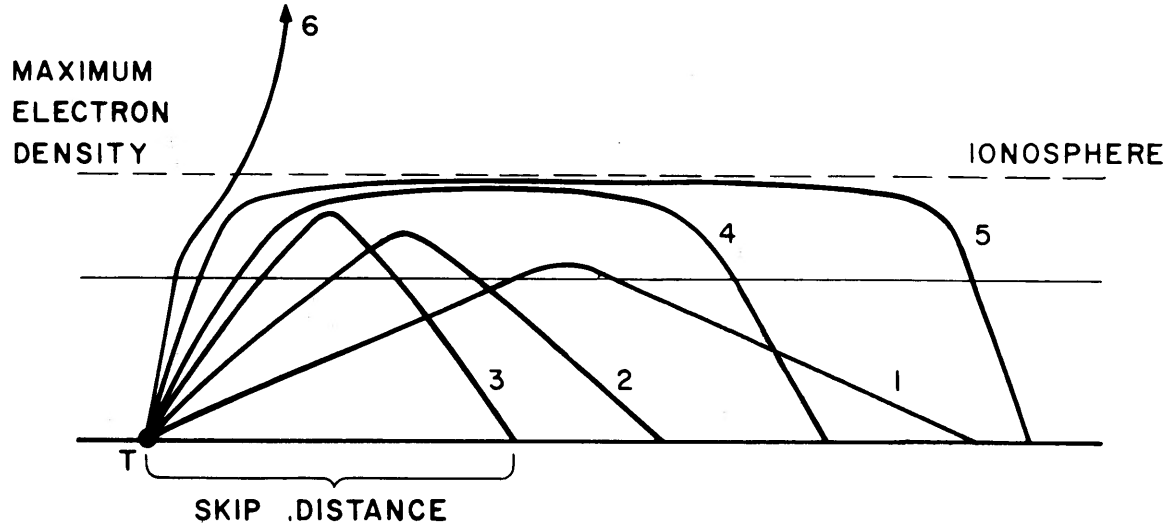


Figure 2-3. Ray Paths for a Fixed Frequency with Varying Angles of Incidence

slight penetration of the layer. As the angle of incidence decreases (rays 2 and 3), penetration into the layer increases and the ground range decreases until an angle of incidence is reached at which the distance is a minimum (ray 3). This minimum distance, called the skip distance, represents the minimum distance from the transmitter at which a sky wave of a given frequency will be returned to earth by the ionosphere. As the angle of incidence is decreased further, the ground range at first increases (rays 4 and 5) and then, eventually, the wave penetrates the layer (ray 6).

The upper, or Pedersen rays, rays 4 and 5 in figure 2-3, are usually not of great practical importance since the field intensity at the ground receiving point is considerably lower than is the case with the lower rays, rays 1, 2 and 3.

2.3.4 Multipath Transmission

A particular propagation path may be pictured as consisting of one or more hops, or successive reflections between the ionosphere and ground. Often more than one path is possible for a given operating frequency and distance. Rays may reach a receiver via two different paths through one layer (an upper and a lower ray), via paths involving two or more layers, via paths corresponding to different numbers of hops, or by combinations of multiple-hop and multiple-layer propagation.

The case of propagation of a radio wave by two layers is illustrated in figure 2-4. For this example, the frequency of the wave is assumed to be such that the E-layer ionization density is sufficient to refract earthward the energy arriving at a large angle of incidence (ray 1) whereas energy arriving at more nearly vertical incidence (ray 2) penetrates the E layer and is returned to earth by the F layer. Although the energy penetrates the E layer its path may be bent considerably as shown by ray 2.

Figure 2-5 illustrates the case of energy reaching the receiver simultaneously from two paths involving different numbers of hops (rays 1 and 2). For average heights of the ionospheric layers, 4000 kilometers is about the maximum great circle distance for one-hop low ray F2-layer propagation, and 2000 kilometers is about the maximum for one-hop E-layer propagation. Greater distance lower ray propagation is possible only by means of two or more hops, as shown by ray 3 of figure 2-5. Abnormal

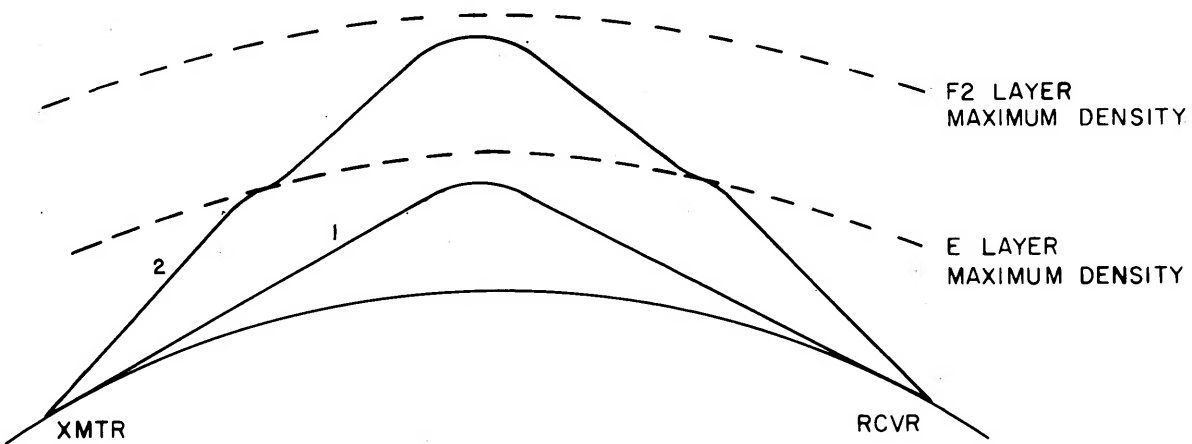


Figure 2-4. Typical Ray Paths with Two Layers Present

ionospheric conditions are sometimes responsible for extended range F2-layer propagation (as great as 10,000 kilometers) without ground reflection, but these ionospheric anomalies are not dependable for long-term planning.

The possible combinations of modes of propagation are virtually unlimited. The E layer may be effective on the daylight side of an east-west path but essentially absent on the nighttime side of the path. Depending upon the frequency and the radiation angle, such a path could include two hops via the F2 layer, it could involve one hop via the E layer and one hop via the F2 layer, or energy could be received via both paths. Usually, the longer the distance and the lower the operating frequency below the MUF, the greater is the number of possible paths.

2.3.5 Multipath and Interference

Since energy may arrive at the receiving terminal by each of several transmission modes, there are differences in time of arrival corresponding to the geometry of the paths. The magnitude and length of these multipath delays depend on combinations of operating frequency, path length, time of day, season, and path location. When an

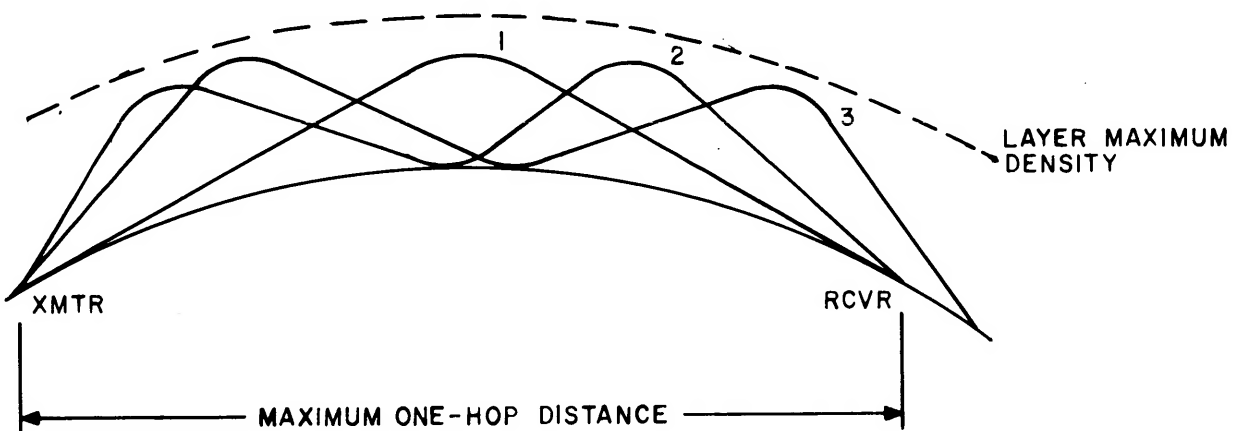


Figure 2-5. Two-Path Transmission

operating frequency very close to the MUF is chosen, the multipath delay is quite short. As the operating frequency is reduced below the MUF, the delay increases up to a maximum for path lengths of approximately 2000 km.

There are two effects of multipath: The first, due to relatively short delays with respect to the signal element length, causes selective fading which affects each subcarrier frequency of a frequency-division multiplex system, in some cases completely destroying the signal element. The second is due to multipath signals that are delayed long enough so that the end of the last arriving multipath signal element interferes with the first arriving component of the next signal element, thus reducing the maximum possible signaling speed. Generally, the delayed signals represent larger numbers of hops and arrive at higher angles than do the more useful signals. Since antenna characteristics of both transmitter and receiver may discriminate in favor of a certain path, suitable antenna design can help to reduce multipath difficulties, but the variability of the ionosphere precludes a complete solution of the problem by this means.

2.4 VARIATIONS IN THE IONOSPHERE

Since the reflecting and absorbing layers of the ionosphere are produced and controlled by radiation from the sun, there is a high correlation between solar activity and ionospheric characteristics. Some of the variations in ionospheric characteristics are more or less regular and can be predicted; other variations, resulting from abnormal behavior of the sun, are irregular and unpredictable.

2.4.1 Regular Variations

a. The Sunspot Cycle. One of the most notable phenomena on the sun's surface is the appearance and disappearance of certain dark areas known as sunspots. Their life-span is variable and their exact nature is not known, but they appear to be vortices in the matter comprising the photosphere (visible surface of the sun). It is known that unusually strong magnetic fields are associated with the sunspots, and since about 1850 it has been known that sunspot activity varies according to a more or less regular cycle. Although there is some variation in the number of sunspots from one maximum to the next and there are some differences in the time between successive maxima, the average sunspot cycle is very close to eleven years.

For many years the index of solar activity has been the smoothed Zurich sunspot number (sometimes referred to as the Wolf number) which is the number of isolated spots plus 10 times the number of groups of spots visible with a standard low-power telescope. Authorities on the subject agree that the validity of the sunspot number as an index of solar activity is questionable. Nevertheless, it is valuable because its availability for a period of about 200 years provides a large homogeneous sample of data.

During times of maximum sunspot activity, the ionization density of all layers increases. Because of this the critical frequencies for the E and F layers increase and absorption in the D layer increases. At these times higher frequencies can be used for long-distance communications; in fact, they must be used to avoid increased absorption of lower frequencies in the D layer.

b. Twenty-Seven Day Cycle. There are periods, particularly near the 11-year minima when a 27-day (approximate) cycle, corresponding to the period of rotation of the sun, is discernible. Magnetic and ionospheric disturbances have been identified frequently with very active sunspots radiating toward the earth at 27-day intervals. Also, as one might expect, rotation of the sun is one factor causing the number of sunspots on the visible surface to change from day to day. This 27-day cycle contributes to the day-to-day variations of the ionosphere over a wide geographic range, but the cycle is neither very predictable nor significant compared to other factors.

c. Seasonal Variations. As the sun moves from one hemisphere to another, variations in the ionosphere take place corresponding to changes in the season. The seasonal variations of the D, E and F1 layers are in phase with the sun's zenith angle; thus the ionization density of these layers is greatest during the summer. The F2 layer, however, does not follow this pattern and its ionization density and height are greatest in winter and least in summer. Separation of the F1 and F2 layers is not as well defined in summer since the F2 layer tends to be lower then.

In the summer, absorption in the ionosphere tends to be linearly related to the sun's zenith angle, but in the winter months the absorption is unexpectedly high. This increased absorption, an effect known as the "winter anomaly," does not occur uniformly over all days, but appears in the form of high absorption on certain groups of days. Apparently, it is a middle latitude effect since it vanishes in polar regions where, in winter, the D region is in prolonged periods of darkness. Fortunately, the winter anomaly is not a serious factor concerning radio communications because the critical frequencies of the F2 layer are higher in winter than in summer, so that higher frequencies can be used. The decrease in absorption due to the use of higher frequencies usually more than compensates for the increased absorption due to the "winter anomaly."

d. Diurnal Variations. The diurnal, or daily, changes in the ionosphere have been discussed in connection with the description of the layers. To summarize here, the salient characteristics are (1) the D, E and F1 layers virtually disappear at night, their ionization density correlating with the altitude of the sun, (2) likewise, the critical frequencies of the E and F1 layers depend primarily on the zenith angle of the sun, and hence follow a regular diurnal cycle, being maximum at noon and tapering off on either side, and (3) the F2 layer exists continuously and its degree of ionization undergoes appreciable, unpredictable day-to-day variations.

2.4.2 Irregular Variations

In addition to the more or less regular variations in the characteristics of the ionosphere, a number of transient unpredictable phenomena have an important, sometimes drastic, effect on HF radio propagation. Some of the more prevalent of these phenomena are: sporadic E, sudden ionospheric disturbances, and ionospheric storms.

a. Sporadic E. Irregular cloud-like areas of unusually high ionization, called sporadic E and abbreviated E_s , often occur near the height of maximum ionization of the regular E layer. The physical processes that produce the quite unpredictable E ionization are not fully known, but the frequency of occurrence and the degree of ionization vary significantly with latitude.

Sometimes the E_s layer, or cloud, is opaque to radio waves and blankets the upper layers. At other times the E_s may be so thin that, although its presence can be verified, radio waves penetrate it easily to be returned to earth by the upper layers. These characteristics can be either helpful or harmful to radio communications. For example, blanketing E_s may block propagation via a more favorable regular layer in a certain frequency range or cause additional attenuation at other frequencies. Partially reflecting E_s can cause serious multipath interference especially detrimental to data transmission systems. On the other hand, sporadic E may enable long-distance transmission at very high frequencies, or may permit short-distance transmission to locations that would ordinarily be in a skip zone.

b. Sudden Ionospheric Disturbances. At times, high-frequency sky-wave transmission over the daylight hemisphere of the earth is "blacked out" by what is known as a sudden ionospheric disturbance (SID). This is the most startling of all the irregularities of the ionosphere since its sudden onset often leads radio operators to believe that their radio receivers have suddenly gone dead. Such a disturbance may last from a few minutes to several hours. The effect is caused by a solar burst of ultra-violet light (solar flare) which is not absorbed in the normal F2, F1 and E layers, but it produces intense ionization in the D region where the air density is relatively high. This results in almost complete absorption of waves above 1 or 2 MHz passing through the D region. The frequency of occurrence of these radio fadeouts is related to the 11-year cycle of flares and sunspots, and the magnitude of an SID generally corresponds with the solar zenith angle.

c. Ionospheric Storms. Ionospheric storms are disturbances in the ionosphere that are associated with magnetic storms, the rapid and excessive fluctuations that occur in the earth's magnetic field. They tend to develop rather suddenly, and recovery to normal conditions may span several days. These storms show a tendency to recur at 27-day intervals, as mentioned earlier, and are associated with sunspots in some manner not fully understood.

The most prominent features of ionospheric storms are an abnormal decrease in F2-layer critical frequencies and an increase in D-layer ionization, and hence absorption. The effects on the E and F1 layers are usually less pronounced. The practical consequence of an ionospheric storm on high-frequency radio transmission is the narrowing of the range of frequencies that are useful for communication over a given circuit. An unusually severe storm may make all high frequencies unusable. The effect of an ionospheric storm tends to be more severe when the transmission path passes near the earth's magnetic pole.

2. 4. 3 Effect of the Earth's Magnetic Field

The earth's magnetic field exerts a deflecting force on the electrons in the ionosphere causing them to vibrate in elliptical paths when they are under the influence of a radio wave. A plane polarized wave becomes elliptically polarized as it travels through the ionosphere. The degree of polarization change is greater the lower the frequency and also depends upon the relative orientation of the magnetic flux lines with respect to the plane of polarization of the wave. When the earth's magnetic field is perpendicular to the electric field of the radio wave, the effect is maximum; when the two fields are parallel, there is no effect.

The magnetic field is also responsible for an effect, called magneto-ionic splitting, whereby a radio wave is split into two components, an ordinary ray and an extraordinary ray. Generally, these rays are elliptically polarized with opposite senses of rotation and refracted along slightly different paths by the ionosphere. The adverse effects of this action are important at frequencies below about 3 MHz and in low-latitude regions.

2.5 TRANSMISSION LOSSES

Three main mechanisms account for almost all the energy losses of a radio transmission: free-space loss, ground reflection loss and absorption loss in the ionosphere. These losses are discussed briefly below, and the method of accounting for transmission losses as a part of HF circuit planning will be shown later in an example problem.

2.5.1 Free-Space Loss

Normally, the major energy loss is due to the geometrical spreading of the energy over progressively larger areas as the signal travels away from the transmitter. For practical purposes, it is sufficiently accurate to consider that this free-space loss causes signal power to diminish in proportion to the inverse square of the ray path distance.

2.5.2 Ground Reflection Loss

When a multiple-hop propagation mode is the means of transmission, energy is lost as the radio wave is reflected at the earth's surface. This loss depends upon the frequency, the angle of incidence, ground reflection irregularities, and the conductivity and dielectric constant of the ground at the reflecting surface.

2.5.3 Absorption Loss in the Ionosphere

As a radio wave propagates into the ionosphere, the electric field vector of the wave produces a force on the free electrons in the atmosphere, setting them into vibration. The resonant frequency of this vibration is known as the gyrofrequency. Except for energy lost by collisions between these electrons and other particles, the electrons release the energy acquired from the radio wave by radiating spherical waves of the same frequency as the original wave. Even though the gas pressure in the ionosphere is very low, the electrons will from time to time collide with gas molecules. When this happens the kinetic energy the electron has acquired from the radio wave is lost insofar as the radio wave is concerned. The amount of energy absorbed in this way from a radio wave depends upon the gas pressure (likelihood of a vibrating electron colliding with a gas molecule) and upon the velocity the electron acquires in its vibration (energy lost per collision), as well as the number of electrons. Consequently, most of the absorption loss occurs in the D region and the lower edge of the E layer where the atmospheric pressure is greatest. Normally, very little loss occurs higher in the ionosphere because the atmospheric pressure is very low. The absorption loss tends to decrease as the frequency is increased because the average velocity of the electrons, and therefore the energy lost per collision, is inversely proportional to frequency.

2.6 NOISE

In every communications system noise is the limiting factor that determines whether the signal is usable for the transmission of information. The three major sources of radio path noise with which the HF signal must compete are galactic, atmospheric and man-made. In general, the composite noise level from these three sources decreases with increasing frequency.

2.6.1 Galactic Noise

The term galactic noise is used loosely here to describe noise generated in outer space, that is, noise from all extraterrestrial sources including our own stellar system, the Milky Way, other galaxies, and so on. The distinctions between cosmic, galactic and solar noise are not important to this discussion but may be pursued further in reference 8.

2.6.2 Atmospheric Noise

The term atmospheric noise is used to designate earth-bound or terrestrial noise generated by natural phenomena. The largest portion of this noise is generated by electrical discharges in the atmosphere. Generally, the level of this "static" decreases with increasing frequency and latitude, and is of minor significance above about 20 MHz.

2.6.3 Man-Made Noise

Man-made noise arises from electrical devices such as relays, voltage regulators, arc-welders, diathermy machines and ignition systems of internal combustion engines. Consequently, man-made noise is especially strong in cities and particularly in industrial areas. Such noise is frequently cyclic in nature because of the periodicity of the generating devices, and it may vary in intensity throughout the working day.

2.6.4 Composite Noise Level

Man-made noise is frequently the performance limiting factor at HF radio receiving sites where urban or suburban encroachment has become a problem. In the absence of man-made noise, atmospheric noise is usually the factor that determines the minimum usable signal. The tremendous energy released by electrical discharges in the atmosphere is transmitted over considerable distances by the same propagating mechanism as is a high-frequency radio signal. Thus the intensity of atmospheric noise or static follows propagation conditions, being high when conditions are favorable for long-distance propagation, and low when propagation conditions are such that the only static able to reach the receiver is that which is generated locally.

In figure 2-6, atmospheric noise curves extracted from CCIR Report 322 have been added to a graph from references commonly used for estimating man-made and galactic noise to illustrate the relative magnitude of the three basic noise sources. The advantage of a rural site is clearly evident as is the inverse relationship between frequency and noise.

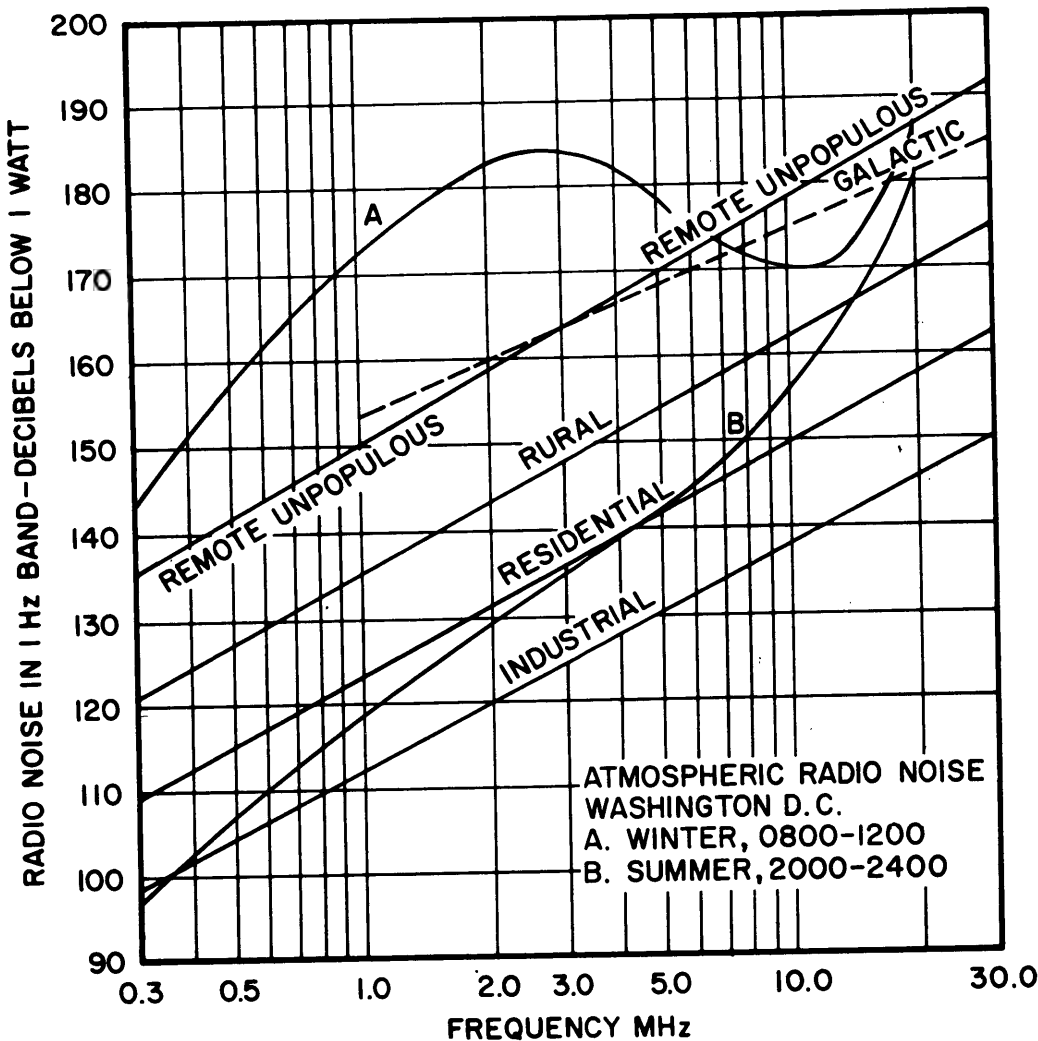


Figure 2-6. Typical Man-Made, Galactic, and Atmospheric Noise

2.6.5 Lowest Usable Frequency (LUF)

Both noise and ionospheric absorption increase with decreasing frequency. Consequently, for a given transmitter output power, as the operating frequency is decreased the signal power at the receiver usually decreases; the noise increases causing the signal-to-noise ratio to deteriorate and the circuit reliability to decrease. The frequency below which the reliability is unacceptable is called the lowest usable frequency (LUF). The LUF depends upon transmitter power, the factors that determine the path loss (e.g., frequency, season, number of hops, geographic location), and the noise level (mainly frequency and receiver location). One of the main factors is ionospheric absorption, and, since this normally varies with the sun's elevation angle, the LUF peaks around noon. The LUF at midday may be higher than the FOT for other times of the day.

2. 6. 6 Required Signal-to-Noise Ratio

The probability of successful HF sky-wave communications depends upon the probability of the operating frequency being supported by ionospheric refraction and the probability that the signal-to-noise ratio will exceed some acceptable level. An acceptable signal-to-noise ratio depends, in turn, upon the type of signal being transmitted, i. e., the type of service. Determining the S/N required for a particular type of service has often been based solely on past experience with the same or similar transmission mode. In recent years, investigations by various agencies have resulted in diverse recommendations concerning the signal-to-noise ratios required for various types of service under both stable and fading conditions. Reference 22 contains useful background information on this subject and includes the recommendations of the Institute for Telecommunication Sciences, Boulder, Colorado.

2. 7 MANUAL PROPAGATION PREDICTIONS

Various kinds of ionospheric propagation predictions are issued monthly by laboratories in a number of different countries. In the United States, the Institute for Telecommunication Sciences (ITS) issues forecasts of ionospheric disturbances and a monthly brochure, "Basic Radio Propagation Predictions," which includes a three-month forecast for use in determining optimum frequencies for HF communications. These relatively short-term predictions are useful in circuit operation, but not for the planning of terminal installations.

For long-term planning, the more predictable characteristics of the ionosphere are relied upon in anticipating the general performance that may be expected for a particular propagation path during a complete sunspot cycle. From this prediction can be drawn the complement of frequencies and radiation angles that will make optimum use of the path as well as the effective radiated power needed to produce a useful signal at the receiving terminal.

The behavior of the E and F1 layers is so regular that permanent nomograms can be used for long-term predictions. On the other hand, the behavior of the F2 layer is very irregular, and data accounting for variations as a function of geography, the time of day, the season and the sunspot number must be used. Therefore, long-term predictions for the F2 layer are based on data for the seasonal extremes (June and December) at a high point and a low point in the solar cycle. For design purposes, NAVELEX uses sunspot numbers 10 and 100 as representative of the normal excursions of conditions associated with solar activity.

The general computational procedure involves the assumption that the ionospheric layers are concentric with the earth's surface and that ionospheric conditions over a path are approximated by conditions at certain reflection areas or control points. For distances up to 4000 kilometers — the normal maximum one-hop distance via the F2 layer — a control point at the midpoint of the path is assumed. For path distances greater than 4000 kilometers, ionospheric conditions are examined at control points 2000 kilometers from each end of the path, and certain mid-path information is added to give an adequate estimate of absorption along the path. Experience has shown that the two-control point method gives useful results, although it ignores the details of propagation between the control points. The method is sometimes used for the E layer also by including an additional pair of control points 1000 kilometers from each end of the path. However, there is less justification for this course than is the case with F2 propagation.

2. 7. 1 Great Circle Path Computations

Knowledge of the transmitter and receiver locations is basic to any propagation prediction problem. The geographic coordinates of the terminal ends of a path can be taken from any standard map having sufficient detail and accuracy so that the coordinates can be determined to the nearest degree. Then, using these coordinates, the shorter of the great-circle distances between the terminals and the bearing from each terminal to the other may be calculated. Estimating the distance with a world map in conjunction with a great-circle map is sufficient for propagation predictions, but, ultimately, a mathematical method must be used to determine the distance to within 5 kilometers and the bearing to within 0.1 degree.

A computer can solve the spherical trigonometry problem quickly, but the manual method is somewhat tedious and time consuming. The formulas and sample problems can be found in a number of texts and handbooks such as reference 20.

2. 7. 2 Calculations for Path Distances of 4000 km or Less

In this section, a path between Cincinnati, Ohio, and Baton Rouge, Louisiana, will be used as an example to discuss the manual procedures for predicting the general performance for path lengths of 4000 kilometers or less. The example is foreshortened by performing the operations for only the month of June at sunspot number 10. As mentioned earlier, the complete solution requires repetition of the procedure for the month of June at SSN 100 and for the month of December at sunspot numbers 10 and 100.

To pose a problem, assume that the circuit will be used for single-sideband suppressed carrier telephony and that the service must be of good commercial quality with 90 percent circuit reliability. The transmitter and the antennas have not been selected. Find the combination of transmitter output power and antenna gains required to provide the service specified.

The graphic materials needed to solve the problem will be found in appendix A, and three foldout worksheets at the end of the handbook are used to illustrate a method and sequence of recording data. Line numbers are continued in sequence from one worksheet to the next to facilitate cross referencing in the step-by-step instructions given below.

a. Record Basic Data

Step 1. From a map or records determine the coordinates of the terminals and record them on the worksheet, foldout 2-1.

Step 2. Place transparent paper over the world map, figure A-1. (The world is divided into three geomagnetic zones, E, I, and W, to take into consideration the variation of F2-layer characteristics with longitude.)

Step 3. Draw the equator and the 0° and 180° meridians on the transparency and label them.

Step 4. Place dots on the transparency at the geographic coordinates of the transmitter and receiver.

Step 5. Transfer the transparency to the great-circle chart, figure A-2, and, keeping the equators coincident, slide the transparency horizontally until the terminal locations lie on the same great circle (solid lines) or a proportionate distance between adjacent great circles.

Step 6. Sketch the great-circle path on the transparency.

Step 7. If the path distance has not been calculated, use the broken lines to estimate the path distance and record it on the worksheet, foldout 2-1.

Step 8. Mark the midpoint of the path on the transparency and record the coordinates in the worksheet heading.

Step 9. Record the geomagnetic zone of the path midpoint.

Step 10. Transfer the transparency to the map of geomagnetic latitudes, figure A-3, and read the geomagnetic latitude of the path midpoint. Record this on the worksheet heading.

Step 11. Transfer the transparency to the world map of E-region gyrofrequency, figure A-4, and read and record the gyrofrequency at the path midpoint.

For the individual line entries on the worksheet the detailed instructions are:

Line 1. MIDPATH LOCAL TIME. Divide the longitude of the path midpoint by 15. Add the quotient to, or subtract it from, the GMT depending upon whether the midpoint is east or west of Greenwich, and then adjust the result to within the normal 24-hour day.

Line 2. F2-ZERO MUF. Place the transparency on the F2-ZERO MUF prediction chart for June, SSN 10, and Zone W (figure A-5). With the equators carefully aligned, place the Greenwich meridian of the transparency on the 00 local time line of the chart and read and record the MUF at the path midpoint. Move the Greenwich meridian of the transparency to the 02 local time line of the chart and again read and record the MUF at the path midpoint. Continue in this manner to complete the tabulating of the F2-ZERO MUF for the even hours of the day. (These are median values for the month.)

Line 3. F2-4000 MUF. Repeat the procedure described for line 2 using the transparency and the F2-4000 MUF chart for June, SSN 10, Zone W (figure A-6).

Line 4. SUN'S ZENITH ANGLE. Place the transparency over the sun's zenith angle chart for June (figure A-7), and, following the procedure described for line 2, read and record the sun's zenith angle for each time block. If the sun's zenith angle exceeds 102 degrees, enter a dash on line 4.

Line 5. ABSORPTION INDEX, I. The ionospheric absorption index, I, is a function of solar activity and the zenith angle of the sun. Enter the nomogram of ionospheric absorption index (figure A-8) with the sunspot number (10 in this case) and the sun's zenith angle from line 4 to determine the absorption index at the path midpoint for each time block.

b. Determine MUFs and FOTs for the Path

3 The next step is to determine the optimum traffic frequencies for the path. Continuing with the worksheet, foldout 2-1, the instructions for each line entry are:

Line 6. F2-MUF. Use the F2-layer MUF conversion nomogram (figure A-9) to determine the MUFs for the path distance. Place a straightedge between the F2-ZERO MUF (line 2) and the F2-4000 MUF (line 3) and read the frequency at the point where the straightedge intersects the vertical line corresponding to the path distance. Repeat the procedure for each time block.

Line 7. F2-FOT. Either multiply each MUF on line 6 by 0.85 or use the conversion scale on the right-hand side of figure A-9 to convert the maximum usable frequencies to optimum traffic frequencies.

Line 8. E-2000 MUF. Use the nomogram for obtaining E-layer 2000 MUF (figure A-10). Enter the nomogram with the sunspot number and the sun's zenith angle from line 4. Read and record the E-2000 MUF for each time block.

Line 9. E-MUF. Enter the F1 and E-layer MUF conversion nomogram (figure A-11) with the path distance and the E-2000 MUF from line 8. Read and record the path E-layer MUF for each time block. Ordinarily the overall path distance is used without regard to the possible number of hops in the path. In a case such as this, however, a one-hop E mode can be ruled out since 2000 km normally is the maximum one-hop distance for E-layer propagation. Therefore, half the path distance is used in this example to determine the E-MUF for a two-hop E mode.

Line 10. CIRCUIT FOT. Enter the higher of the F2-FOT (line 7) or the E-MUF (line 9).

A curve may now be drawn to portray graphically the median optimum traffic frequencies for the month of June, SSN 10. Such a curve for the example problem is shown in figure A-12.

c. Determine Possible Modes

For clarity and convenience, the example is further abbreviated at this point to show the procedures for only one time, 1200Z. Usually the work described is done for 4-hour intervals through the day. Foldout 2-2 is used with reference to the following instructions for entries to be made on each line. Enter heading information from the previous worksheet.

Line 11. OPERATING FREQUENCY. At this point an operating frequency must be designated for the time 1200Z. If a complement of frequencies has been assigned for the circuit, the highest one below the FOT is a reasonable first choice. Otherwise enter the FOT from the preceding worksheet.

Line 12. F2-LAYER HEIGHT. Place the great-circle path transparency on the F2-layer height chart for June (figure A-13), and, with the equators and the Greenwich meridian of the transparency on the 1200 local time line, read and record the layer height at the path midpoint.

Line 13. MODES CONSIDERED. No entry required. The modes to be considered for paths of 4000 kilometers or less are already entered on line 13. 1E indicates one hop via the E layer; 2F indicates two hops via the F layer, etc.

Line 14. DISTANCE PER HOP. Divide the path distance (in the data sheet heading) by the number of hops in line 13.

Line 15. RADIATION ANGLE Δ . The vertical radiation angle corresponding to each mode is obtained from figure A-14 which gives the radiation angle as a function of great-circle distance and layer height. Enter with the distance per hop (line 14) and a layer height of 110 km for the E modes and with distance per hop and F2-layer height (line 12) for the F modes.

Line 16. MAXIMUM E Δ , MINIMUM F Δ . The maximum possible radiation angle for E-layer propagation (the critical angle) is obtained from figure A-15, "Nomogram to Estimate E-layer Penetration Frequency at any Radiation Angle." Enter with the operating frequency from line 11 and the absorption index from line 5. If the radiation angle for either of the E modes, as recorded on line 15, is greater than the maximum possible radiation angle entered on line 16, eliminate that mode from further consideration. Since F-layer propagation requires penetration of the E layer, the minimum vertical radiation angle for the F layer is considered to be the same as the maximum radiation angle for the E layer. Therefore, eliminate any F modes for which the radiation angle on line 15 is less than the minimum radiation angle on line 16.

Line 17. MINIMUM F DISTANCE. Enter figure A-9 with the F2-ZERO MUF from line 2 and the F2-4000 MUF from line 3. At the operating frequency (line 11), read the minimum distance (skip distance) for F2-layer propagation. If this distance is greater than any of the distances per hop shown for F modes on line 14, eliminate those modes from further consideration.

If all the F modes are eliminated because of the line 15 radiation angle limitations, introduce additional modes by increasing the number of hops. If all modes are eliminated, and the operating frequency is below the FOT, introduce a combination E and F layer mode (EF mode) using the average of 110 km and the F-layer height (line 12).

d. Estimate Path Loss

Line 18. IONOSPHERIC LOSS PER HOP. The average absorption loss per hop is obtained from the ionospheric absorption nomogram (figure A-16). Enter with the absorption index from line 5 and the radiation angle from line 15 for the path being considered. Mark the center line of the nomogram. Add the gyrofrequency, from the data sheet heading, to the operating frequency. A line from this sum on the right-hand scale, through the point previously marked on the center line, to the left-hand scale yields the absorption loss per hop.

Line 19. TOTAL IONOSPHERIC LOSS. Multiply the ionospheric loss per hop on line 18 by the number of hops, line 13.

Line 20. GROUND LOSS PER REFLECTION. The loss at each ground reflection is estimated from the appropriate reflection loss chart (figure A-17 or A-18). Select the chart most nearly approximating the terrain at the path midpoint, either ground or sea water. Enter the operating frequency and the radiation angle, line 15, and read the ground reflection loss.

Line 21. TOTAL GROUND LOSS. Multiply each ground loss on line 20 by the number of ground reflections (the number of hops minus one) to get an estimate of total ground reflection loss.

Line 22. RAY-PATH DISTANCE LOSS. Loss due to spreading of the radio energy as it travels is obtained from the nomogram of figure A-19. Enter with the path distance from the worksheet heading and the radiation angle from line 15. Mark the reference line. Enter with the reference mark and the operating frequency and read the distance loss. Repeat the procedure for each mode still being considered.

Line 23. QUASI-MINIMUM PATH LOSS. The lowest hourly median path loss that normally can be expected is estimated by adding lines 19, 21, and 22.

Line 24. ADJUSTMENT TO MEDIAN. The difference between the quasi-minimum path loss (lowest hourly median loss expected within the month) and the monthly median of the hourly median can be estimated from figure A-20. Determine the appropriate curve according to the geomagnetic latitude of the path midpoint (recorded on foldout 2-1) and read the path loss adjustment at the median (50%) ordinate.

Line 25. MEDIAN PATH LOSS. Add the entry in line 24 to the lowest entry in line 23 to obtain the expected monthly median of the hourly median path loss.

Line 26. ADJUSTMENT FOR 90% SERVICE. This adjustment is obtained from figure A-21, "Daytime Reliability of Sky-Wave Circuits below 60° Geomagnetic Latitude." Read the reliability correction expressed in decibels at the intersection of the operating frequency with the 90% contour. The 90% contour is used because Navy standard practice is to design for a circuit reliability of at least 90%.

Line 27. PATH LOSS FOR 90% SERVICE. Add the entries on lines 25 and 26.

e. Estimate HF Noise at the Receiver Location

An estimate of the high-frequency radio noise is required before the signal requirement, and ultimately the radiated power and path antenna gain, can be determined. Foldout 2-3 is used to continue with the abbreviated example begun on the path loss worksheet. Heading information is taken from the other worksheets. The instructions for the line entries are:

Line 28. LOCAL TIME. Divide the longitude of the receiving terminal by 15. Add the quotient to, or subtract it from, the GMT, depending upon whether the receiving terminal longitude is east or west of Greenwich, and then adjust the result to within the normal 24-hour period.

Line 29. F2-ZERO MUF. Transcribe the F2-ZERO MUF from line 2.

Line 30. 1 MHz NOISE LEVEL. To estimate the noise in dB above kT_b at 1 MHz, use the noise distribution chart (figure A-22) and read the noise level at the receiver location. Local time is the basis for selecting the appropriate chart from the series presented in reference 9.

Line 31. ATMOSPHERIC NOISE, 1-Hz BANDWIDTH. Use the atmospheric radio noise chart (figure A-23). Enter with the operating frequency and the 1-MHz noise level from line 30. Read and record atmospheric noise.

Line 32. GALACTIC NOISE. Galactic noise will be important only if the operating frequency is above the critical frequency of the F2 layer in the receiving vicinity. This critical frequency is approximated by the F2-ZERO MUF. If the operating frequency is below the F2-ZERO MUF, line 29, enter a dash on line 32. If the operating frequency is above the F2-ZERO MUF enter figure A-24 with the operating frequency and read the galactic noise.

Line 33. MAN-MADE NOISE. If at all possible, measurements of man-made noise should be made for each individual case, but if measurements at the receiving site are not available, man-made noise may be approximated from figure A-24. Enter with frequency and read noise from the curve most typical of the receiving location. A rural location is assumed for the sample problem.

Line 34. NOISE AT RECEIVING ANTENNA, 1-Hz BANDWIDTH. Enter the highest of the entries in lines 31, 32 and 33.

f. Estimate Power Required

Continuing on with foldout 2-3, the following instructions lead to an estimate of the path effective radiated power required; that is, the combination of transmitter power and antenna gains required to overcome the path loss and provide an acceptable signal-to-noise ratio.

Line 35. NOISE, 3-kHz BANDWIDTH. Since the noise level in line 34 is for a 1-Hz bandwidth, a correction must be made to express the noise in the bandwidth occupied by the signal, 3-kHz. Add 35 dB (10 log 3000, rounded off) algebraically to the 1-Hz noise power in line 34.

Line 36. REQUIRED S/N. For this problem the ITS recommendations of reference 22 were adopted and it was assumed that dual diversity would be employed. Reference 22 recommends 67 dB as the signal-to-noise ratio required for good commercial quality SSB suppressed carrier telephony under fading conditions with dual diversity. This value, which is referenced to noise in a 1-Hz band, must be corrected for the actual bandwidth of the noise, 3 kHz. Subtracting 35 dB yields 32 dB as the required signal-to-noise ratio.

Line 37. SIGNAL REQUIRED. Record the algebraic sum of lines 35 and 36.

Line 38. PATH LOSS FOR 90% SERVICE. Enter the value from line 27.

Line 39. PATH EFFECTIVE POWER. Add lines 37 and 38 algebraically to obtain the combination of transmitter power (at the antenna terminals) and transmitting and receiving antenna gains required. With the effective power determined for the type of service and circuit reliability required, a trade-off between transmitter power and path antenna gain can be made to lead to selection of the transmitter and the antennas. Usually, the simplest and most economical way to contribute power to a circuit is by using high gain antennas.

2.7.3 Calculations for Path Distances Greater Than 4000 km

It should be clearly evident from the abbreviated example above that the work of making HF radio path performance predictions is quite tedious when it is done manually. To continue on with an example for a path length greater than 4000 kilometers would simply add to the bulk of this handbook while contributing very little more to a basic understanding of the computational procedure. Those who desire to investigate manual computational procedures more thoroughly should refer to the literature on the subject. The method for paths greater than 4000 kilometers generally follows that described for the short path, except additional control points are used. These control points introduce some additional minor complications.

2.8 COMPUTER PROPAGATION PREDICTION PROGRAMS

A technique called numerical mapping is used in computer programs to tabulate and store basic ionospheric data. With this technique, a table of numerical coefficients is used to define a function of latitude, longitude and time to produce a "numerical map" of an ionospheric characteristic. The resultant numerical map represents the world-wide and diurnal variations of a particular characteristic, for example, the median F2-ZERO MUF for a given month. Numerous tables of coefficients can be calculated and stored in a computer for use on demand in predicting ionospheric characteristics for many variations of season and solar activity. As new data become available, the coefficients can be easily revised using the computer.

In a computer program, all the computations described in the example illustrating the manual procedures (and a few more) are made by the computer for each hour at 1 MHz intervals from 2 to 30 MHz. For each hour and for each frequency, seven possible modes are chosen: three F modes, two E modes, and two EF modes. For each of the seven possible modes the probability of ionospheric support is calculated, and the mode with the highest value is chosen as the most probable mode. There are various options that can be exercised concerning the output data to be printed. For example, the mode, radiation angle, transmission delay for the most probable mode, probability of ionospheric support via at least one sky-wave path, signal-to-noise ratio at the receiving antenna terminals and system loss are illustrative of the types of data that can be supplied. The particular mix of output data printed depends upon the input parameters specified and upon the desires of the user of the data. The computer printouts used by NAVELEX omit much of the optional data in order to reduce the bulk of the data to that which is essential for radio link and antenna design purposes.

Two basic approaches are used by NAVELEX for obtaining ionospheric prediction data via a computer. In one case, the transmitter power and antenna gains are specified (among other parameters) and the computer printout gives the radiation angle and circuit reliability. For the other approach, the reliability is specified and the computer prints the radiation angle and the power required.

a. Reliability Prediction Program. Figure 2-7 shows a computer printout for a specific circuit giving the radiation angle and circuit reliability at 1-MHz intervals for each hour of the day. The heading entries from left to right are:

CIRCUIT NO.	JUNE												SUNSPOT NO. 10												
	TO SAN MIGUEL			AZIMUTHS			N.MI.			KM.			TO BARRIGADA			AZIMUTHS			N.MI.			KM.			
	13°45'N = 144°49'E	14°45'N = 144°49'E	14°45'N = 144°49'E	276.7	90.5	144.3	2673.0	RCVR ANT GAIN	15(DA)	144.3	2673.0		13°45'N = 144°49'E	14°45'N = 144°49'E	14°45'N = 144°49'E	276.7	90.5	144.3	2673.0		RCVR ANT GAIN	15(DA)			
1	0.65	0.45	0.99	0.99	0.99	0.99	0.99	0.99	0.99	0.99	0.99	0.99	0.78	0.63	0.47	0.37	0.28	0.20	0.14	0.09	0.05	-	-	-	
2	0.5	0.5	0.5	0.5	0.5	0.5	0.5	0.5	0.5	0.5	0.5	0.5	0.8	0.8	0.8	0.8	0.8	0.8	0.8	0.8	0.8	0.8	-	-	-
3	0.80	0.72	0.98	0.99	0.99	0.99	0.99	0.99	0.99	0.99	0.99	0.99	0.77	0.62	0.46	0.36	0.27	0.20	0.13	0.09	0.05	-	-	-	
4	0.77	0.71	0.98	0.99	0.99	0.99	0.99	0.99	0.99	0.99	0.99	0.99	0.84	0.72	0.56	0.44	0.34	0.26	0.16	0.13	0.08	0.05	-	-	-
5	0.71	0.61	0.97	0.99	0.99	0.99	0.99	0.99	0.99	0.99	0.99	0.99	0.79	0.65	0.49	0.40	0.31	0.23	0.17	0.12	0.08	-	-	-	
6	0.80	0.92	0.98	0.99	0.99	0.99	0.99	0.99	0.99	0.99	0.99	0.99	0.77	0.7	0.58	0.47	0.37	0.28	0.20	0.14	0.09	0.06	-	-	-
7	0.87	0.76	0.90	0.99	0.99	0.99	0.99	0.99	0.99	0.99	0.99	0.99	0.77	0.66	0.56	0.46	0.36	0.28	0.24	0.18	0.12	0.08	0.05	-	-
8	0.28	0.20	0.19	0.18	0.19	0.19	0.19	0.19	0.19	0.19	0.19	0.19	0.6	0.6	0.6	0.6	0.7	0.7	0.7	0.7	0.7	0.7	0.7	0.7	-
9	0.03	0.22	0.38	0.59	0.49	0.96	0.99	0.99	0.99	0.99	0.99	0.99	0.99	0.99	0.99	0.99	0.99	0.99	0.99	0.99	0.99	0.99	0.99	0.99	-
10	0.5	0.23	0.26	0.18	0.17	0.17	0.17	0.17	0.17	0.17	0.17	0.17	0.5	0.5	0.5	0.5	0.5	0.5	0.5	0.5	0.5	0.5	0.5	0.5	-
11	0.05	0.33	0.33	0.33	0.33	0.33	0.33	0.33	0.33	0.33	0.33	0.33	0.99	0.99	0.99	0.99	0.99	0.99	0.99	0.99	0.99	0.99	0.99	0.99	-
12	0.37	0.26	0.18	0.16	0.16	0.16	0.16	0.16	0.16	0.16	0.16	0.16	0.23	0.23	0.23	0.23	0.23	0.23	0.23	0.23	0.23	0.23	0.23	0.23	-
13	0.16	0.05	0.03	0.03	0.03	0.03	0.03	0.03	0.03	0.03	0.03	0.03	0.3	0.3	0.3	0.3	0.3	0.3	0.3	0.3	0.3	0.3	0.3	0.3	-
14	0.18	0.06	0.04	0.04	0.04	0.04	0.04	0.04	0.04	0.04	0.04	0.04	0.81	0.81	0.81	0.81	0.81	0.81	0.81	0.81	0.81	0.81	0.81	0.81	-
15	0.94	0.97	0.98	0.99	0.99	0.99	0.99	0.99	0.99	0.99	0.99	0.99	0.92	0.87	0.82	0.75	0.66	0.57	0.46	0.32	0.20	0.11	0.05	-	
16	0.96	0.98	0.99	0.99	0.99	0.99	0.99	0.99	0.99	0.99	0.99	0.99	0.94	0.94	0.94	0.94	0.94	0.94	0.94	0.94	0.94	0.94	0.94	0.94	-
17	0.94	0.97	0.98	0.99	0.99	0.99	0.99	0.99	0.99	0.99	0.99	0.99	0.92	0.87	0.82	0.75	0.66	0.57	0.46	0.32	0.20	0.11	0.05	-	
18	0.18	0.06	0.04	0.04	0.04	0.04	0.04	0.04	0.04	0.04	0.04	0.04	0.5	0.5	0.5	0.5	0.5	0.5	0.5	0.5	0.5	0.5	0.5	0.5	-
19	0.93	0.96	0.98	0.99	0.99	0.99	0.99	0.99	0.99	0.99	0.99	0.99	0.94	0.94	0.94	0.94	0.94	0.94	0.94	0.94	0.94	0.94	0.94	0.94	-
20	0.16	0.05	0.03	0.03	0.03	0.03	0.03	0.03	0.03	0.03	0.03	0.03	0.77	0.77	0.77	0.77	0.77	0.77	0.77	0.77	0.77	0.77	0.77	0.77	-
c1	0.17	0.59	0.93	0.98	0.99	0.99	0.99	0.99	0.99	0.99	0.99	0.99	0.99	0.99	0.99	0.99	0.99	0.99	0.99	0.99	0.99	0.99	0.99	0.99	-
c2	0.02	0.28	0.91	0.96	0.97	0.97	0.97	0.97	0.97	0.97	0.97	0.97	0.99	0.99	0.99	0.99	0.99	0.99	0.99	0.99	0.99	0.99	0.99	0.99	-
23	0.5	0.23	0.15	0.10	0.09	0.04	0.03	0.04	0.05	0.04	0.04	0.04	0.46	0.32	0.21	0.12	0.06	-	-	-	-	-	-	-	-
24	0.17	0.59	0.93	0.98	0.99	0.99	0.99	0.99	0.99	0.99	0.99	0.99	0.99	0.99	0.99	0.99	0.99	0.99	0.99	0.99	0.99	0.99	0.99	0.99	-

Figure 2-7. Computer Printout for Reliability Prediction Program

PAGE 1

First Line

- (1) sequential number of circuit as entered into machine,
- (2) month of year,
- (3) solar activity level.

Second Line

- (1) transmitter and receiver locations,
- (2) azimuths (forward and backward),
- (3) nautical miles,
- (4) kilometers.

Third Line

- (1) geographic coordinates of transmitter and receiver in hundredths of degrees,
- (2) azimuths from transmitter to receiver and then from receiver to transmitter,
- (3) great-circle distance of path in nautical miles,
- (4) great-circle distance of path in kilometers.

Fourth Line

- (1) transmitting antenna description, or antenna gain.
- (2) receiving antenna description, or antenna gain.

Fifth Line

- (1) off azimuth of transmitting antenna, degrees;
- (2) minimum angle above the horizon for which any mode will be calculated, degrees;
- (3) off azimuth of receiving antenna, degrees.

Sixth Line

- (1) average output power of the transmitter at the antenna terminals,
- (2) measured or assumed man-made noise level at the receiving antenna site in dB relative to 1 watt at 3 MHz in a 1-Hz bandwidth,
- (3) required signal-to-noise ratio (dB)
 - (a) the median signal power required in the occupied bandwidth relative to the noise power in a 1-Hz bandwidth;
 - (b) the signal power required must be the average power to be consistent with the power indicated at the transmitting antenna terminals.

In the body of the printout, GMT is the ordinate and the operating frequency is the abscissa. The radiation angle for the most probable path and the reliability are shown for each frequency and hour. Dashes in a column below a frequency mean that the probability of all sky-wave paths inspected fell below .05. A plus sign indicates that the probability of ionospheric support was greater than .05, but reliability was less than .005.

For the sample shown in figure 2-7, rhombic antennas with a nominal gain of 15 dB were assumed for both the transmitter and receiver sites. For any circuit planning that includes installation of new antennas, zero degrees off azimuth is specified. That is, it is assumed the antennas can be installed on the correct azimuth. A minimum radiation angle of three degrees is commonly specified in recognition of the practical limitations on achieving lower take-off angles. Also, man-made noise at 3 MHz is usually taken from the rural curve of figure A-24 unless measured noise data is available.

It is important to note the effect of the choice between antenna gain and antenna description as an input parameter. Although the computer program can calculate the theoretical directive gain of real antennas, the transmitting and receiving antennas in the example were assumed to have a constant gain (15 dB). This approach offers some advantages over specifying a particular antenna. In the latter case the vertical radiation pattern of the antenna will enter into the computations and the reliability figures will be affected by the variation of antenna gain with radiation angle. As a result, there could be a number of computations indicating excellent path reliability, but, because of insufficient antenna gain at the radiation angle required, the computer printout may show that the path is unreliable. The most probable path might be eliminated in this way. The computer printout does not indicate which unsatisfactory reliability results were due to poor antenna gain, and one cannot see the results of antenna design adjustments except by running the program again with a different antenna specification.

On the other hand, if a constant antenna gain is assumed, the predictions are not affected by any antenna pattern. As far as the computer program is concerned, the antenna gain will be constant, 15 dB in the example, at any radiation angle needed. The antenna design can then be adjusted for maximum gain at the radiation angle most suitable for the path.

Another important point concerns the designation of power and signal-to-noise ratio required. The power specified must be the average power in the occupied bandwidth, and the signal-to-noise ratio required must be adjusted to allow for the fact that the computer program noise computation is for a 1-Hz bandwidth. In the example, the specified signal-to-noise ratio, 59 dB, is the sum of 24 dB, the required signal-to-noise ratio for a signal in a 3-kHz band and noise in a 3-kHz band, and 35 dB, the factor to convert to a signal-to-noise ratio with the signal in a 3-kHz band and the noise in a 1-Hz band as required by the prediction program.

On the sample computer printout, all the circuit reliability figures of 90 and higher have been underlined to give a quick graphic impression of the frequencies and radiation angles appropriate for use at various times throughout the day. For predictions covering a complete solar cycle there would be, in addition to the sheet shown, a printout for June, SSN 100; one for December, SSN 10; and one for December, SSN 100.

b. Power Prediction Program. This program is a relatively recent development sponsored by the Naval Electronic Systems Command and implemented by the ITS. Historically, power was never considered to be a predictable system parameter. Rather, it was treated as one of the system parameters that must be specified prior to the start of the prediction process. In many cases, this was and still is, the direct route to the desired result, namely, the propagation predictions for a specified power. In other cases, however, the desired result is the power required to achieve a given

reliability for a specified class of service. For the latter cases the power had to be determined by a trial and error process involving repetitive computer runs for each set of values for all the variables in question. This wasteful, large expenditure of man-hours and of computer time is avoided by this new program.

Figure 2-8 shows a computer printout for the same circuit as in figure 2-7, this one being for December and SSN 100. This time, however, the reliability (90% on line 6) was specified and the computer program was required to determine the power required to achieve that reliability. In this case isotropic antennas were specified (0 dB gain) and no allowance for signal bandwidth was added to the required signal-to-noise ratio (24 dB). The dashes in the body of the printout have the same meaning as in the previous example, i. e., the probability of ionospheric support was less than 0.05. The double asterisks indicate that the probability of ionospheric support was less than the required circuit reliability, in which case no amount of power will suffice.

As a general observation, this type of printout shows the effect of power on extending the useful frequency range. Note that propagation reliability, rather than power, is the determining factor at the higher frequencies, while power is the controlling factor at the lower frequencies. That is, increasing the power can increase the usable low frequencies, but not the high. This is as one might expect since both noise power and absorption loss increase with decreasing frequency.

The power prediction program offers several advantages over the reliability prediction program for long-term circuit planning, and the choices of input parameters shown in this example (figure 2-8) capitalize on these advantages. Since the required power is expressed in decibels above 1 watt, one can consider it an effective power and can perform easily any desired tradeoffs among transmitter power, antenna gains, required signal-to-noise ratio, and bandwidth. Assuming 0 dB antenna gain further simplifies these tradeoffs since the predictions will not have been affected by any prior assumptions concerning antenna gain.

To relate this example to the previous one, consider the input parameters for figure 2-7 as follows:

Transmitter power: $10 \log 6000$	= 37.8 dBw
Antenna gain, transmit	= 15 dB
Antenna gain, receive	= 15 dB
Effective signal power	= 67.8 dBw
3-kHz noise bandwidth adjustment	= -35 dBw
Available signal power	= 32.8 dBw

From this computation, one can see that the assumed transmitter power and antenna gains will satisfy the circuit reliability requirement for all frequencies and times for which the predicted power requirement is less than 33 dB. As with the previous example, lines drawn under the power predictions, as in figure 2-8, give a quick impression of the range of frequencies usable as a function of time of day. One would expect that assuming the same input parameters for both prediction programs would yield the same set of frequencies from both approaches. This is true. They correspond exactly, although an example of each type of printout for the same month and the same sunspot number would be needed to show this.

Figure 2-8. Computer Printout for Power Prediction Program

As mentioned earlier, the antenna gains specified in the first example and used to relate the second example to the first were arbitrary, though achievable, values. With the power predictions in hand for June and December for each of the two sunspot numbers, 10 and 100, the designer can give serious attention to selecting a practical antenna. An intermediate step is useful, though, to collect data from the four computer printouts into a composite summary for the complete solar cycle.

A convenient format for collecting data from the four computer-printed prediction tables is a simple matrix such as that shown in figure 2-9. Each frequency column of the four prediction tables is examined and all of the radiation angles underlined are indicated for each frequency in the matrix by marks opposite those radiation angles. The example shows the result of collecting data from just the two printouts of figures 2-7 and 2-8. The trend and grouping of required radiation angles as a function of frequency can be seen, but data from the two other tables (not shown) must be added to complete the matrix. When the matrix is completed, the grouping of radiation angles will be evident. The designer can then use a catalogue of standard rhombic antenna designs to select antennas that have adequate gain and vertical radiation patterns that match the radiation angle-frequency pattern of the predictions. Rhombic antennas, two to cover the HF band, are indicated here because they are the most common for long-haul point-to-point circuits, but this is not meant to imply that the procedures described above are restricted to any particular type of antenna.

A note of caution is in order here concerning the use of a radiation angle/frequency matrix as the basis for antenna design. Although the matrix is a very useful adjunct to the prediction tables, figures 2-7 and 2-8, it should not be used as the sole reference for determining the antenna system design. Doing so could lead to an unnecessarily complicated and expensive antenna system that includes performance features beyond those needed. For instance, the sample matrix of figure 2-9, taken by itself, could be interpreted to indicate that the vertical radiation pattern of the antenna system should include three principal lobes aligned with the pattern of radiation angles shown by the matrix. On the other hand, examination of the prediction tables of figures 2-7 and 2-8 shows that the two higher groups of radiation angles can be ignored (at least for the seasons and sunspot number of those computer runs) since there are frequencies that can be used with low radiation angles to maintain communication throughout the day. The matrix must be evaluated in conjunction with the four computer prediction tables (for June and December, and SSNs 10 and 100 for each month) to determine the minimum complement of frequencies and radiation angles that will satisfy the circuit requirements. The result of such an evaluation is illustrated by the dotted line of figure 2-9 which encloses the group of low radiation angles for which the antenna should be designed. The practical aspects of antenna selection or design are discussed in greater detail in NAVELEX 0101, 104 — "HF Radio Antenna Systems."

Propagation path analysis as discussed here is primarily applicable to point-to-point circuits. The same general procedure can be used to determine path requirements for other types of communications, such as ship-to-shore, but the voluminous computations involved limit practical application.

c. LUF-HUF Tables. As a by-product of the power prediction program, the computer can print tables of the LUF (lowest useful frequency) and the HUF (highest useful frequency) for a given circuit reliability. Such a table is shown in figure 2-10. An "x" in the table indicates that the LUF and the MUF do not exist. The frequencies are given in tenths of megahertz, a refinement over the lowest and highest frequencies that would be tabulated by underlining the prediction tables as was done in figures 2-7 and 2-8.

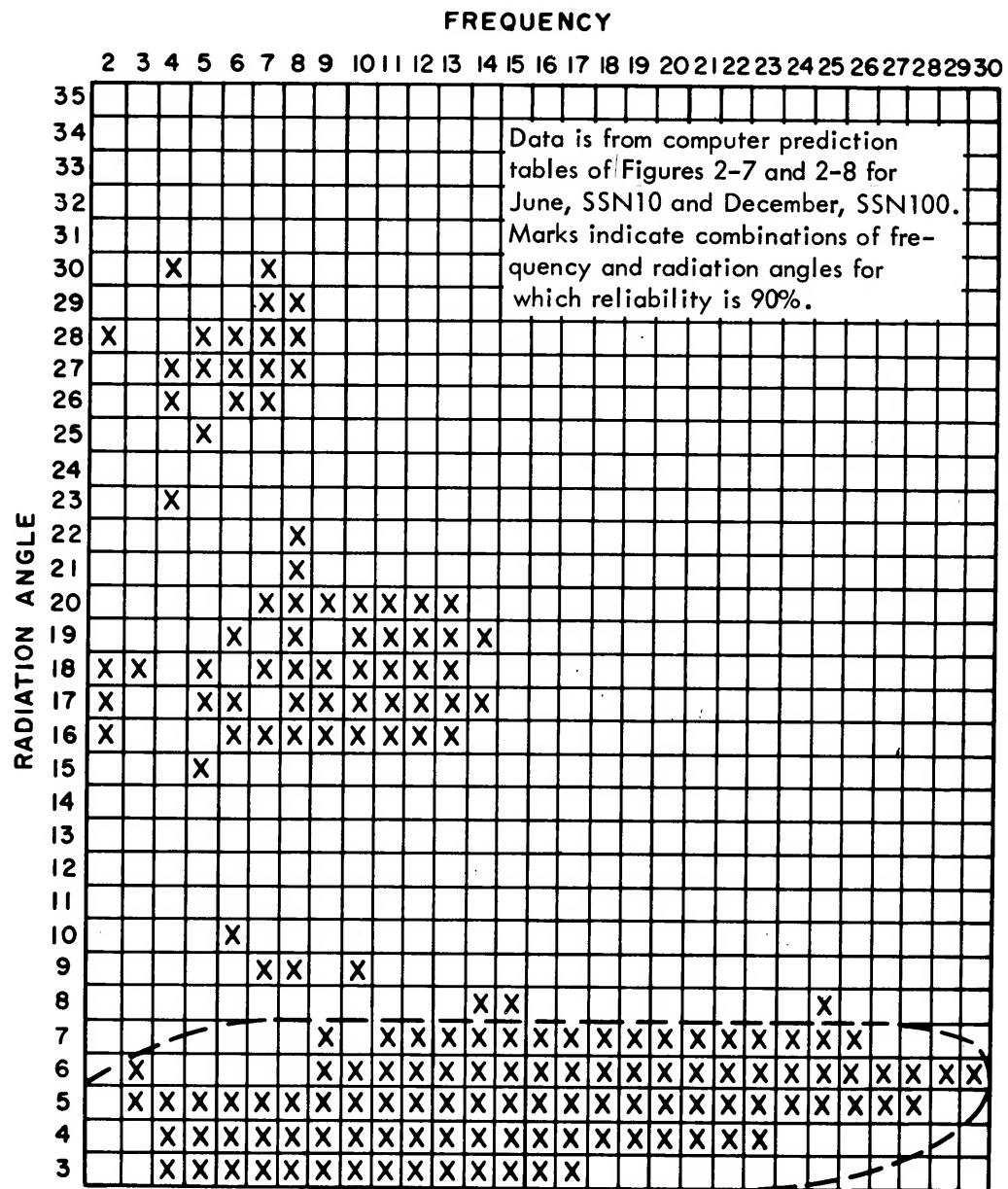


Figure 2-9. Radiation Angle/Frequency Matrix

CIRCUIT NO. 2 ----- JUNE ----- SUNSPOT NO. 10
 MIDWAY TO CLAM LAGOON AZIMUTHS N.MI. KM.
 28.22N - 177.35W 51.90N - 176.70W 1.0 181.4 1422.1 2633.7
 XMTR ANT GAIN 10(DB) RCVR ANT GAIN 10(DB)
 OFF AZIMUTH 0 DEG. MIN. ANGLE= 3 DEG. OFF AZIMUTH 0 DEG.
 PWR= 0.10KW 3 MHZ. MAN. NOISE = -148 DBW REQ.S/N= 59DB

THE LOWEST (L) AND THE HIGHEST (H) 90.0 PERCENT RELIABLE FREQUENCIES VERSUS THE HOUR GMT

GMT	L	H
1	X	X
2	X	X
3	X	X
4	X	X
5	X	X
6	X	X
7	12.2	14.7
8	8.8	15.0
9	7.5	14.0
10	8.1	9.3
11	7.6	8.7
12	7.4	8.2
13	7.4	7.9
14	X	X
15	X	X
16	X	X
17	X	X
18	X	X
19	X	X
20	X	X
21	X	X
22	X	X
23	X	X
24	X	X

Figure 2-10. LUF-HUF Table

